Modal Equivalent Circuit of Bend Discontinuity in Differential Transmission Lines

Yoshitaka Toyota, Shohei Kan, Kengo Iokibe
Graduate School of Natural Science and Technology
Okayama University
3-1-1 Tsushima-naka, Kita-ku, Okayama, Japan
Email: toyota@okayama-u.ac.jp

***Abstract*—The equivalent-circuit expression of bend discontinuity in differential transmission lines, which is derived from the view of the mode-decomposition technique, is proposed in this paper. We investigated the relationship between the amount of mode conversion in the bend region and two components in the modal equivalent circuit: the mode-conversion sources and the modal reactances (modal inductances and capacitances). As a result, it was found that not only the difference in the imbalance factor but also the magnitude of the modal reactances can have a lot of effect on the mode conversion.**

***Keywords*—mode-decomposition technique, modal equivalent circuit, mode-conversion sources, imbalance factor, modal reactance, differential transmission line, bend**

I. Introduction

We can use a modal equivalent circuit created applying the mode-decomposition technique to the telegrapher's equations for analyzing a multi-conductor transmission-line system [1]–[3]. Then, the technique takes on an imbalance factor as a parameter to obtain orthogonal modes [3]. The fundamental multi-conductor transmission-line system is a wave-guiding system composed of two-conductor lines and the system ground, where two orthogonal modes, which are the normal (or differential) and common modes, exist.

Our previously proposed modal equivalent-circuit model with mode-conversion sources, which is based on the mode-decomposition technique, can be used to simulate the conversion caused by discontinuity in a multi-conductor transmission-line system [4]. In the model, the discontinuity in the multi-conductor transmission line corresponds to inequality in the imbalance factors of the transmission line, and then, the magnitude of the mode-conversion sources is proportional to the difference in the imbalance factor. Therefore, the larger the difference in the imbalance factor becomes, the more the magnitude of the mode-conversion sources is increased.

Circuit simulation was carried out to validate the modal equivalent-circuit model with mode-conversion sources, where the current division factor was used as the imbalance factor, by using a simple transmission system where two microstrip lines on a printed circuit board and a parallel two-wire cable are connected [4], [5]. The results obtained from the circuit simulation using the modal equivalent-circuit model were in good agreement with those obtained from full-wave simulation and measurement as long as the TEM-mode propagation was satisfied. In addition, this approach is advantageous because there are less calculation costs and countermeasure consideration compared with full-wave simulation.

In this paper, this approach is applied to bend discontinuity in the differential transmission lines on printed circuit boards. This study will help us to consider a bend structure with less mode conversion. The mode conversion was clarified to be related to not only the current division factor but also the modal characteristic impedance of the transmission line [6]. This paper also investigates the modal reactive elements of the bend, focusing on the imbalance factor of the bend in the differential transmission lines.

II. Modal Equivalent Circuit of Bend Discontinuity in Differential Transmission lines

A. Mode Decomposition with Imbalance Factor

The modal equivalent circuit is taken from the actual circuit by the mode-decomposition technique [1]–[3]. Fig. 1(a) shows coupled transmission lines consisting of conductor line #1 (signal line) and conductor line #2 (return line). In addition, V_1 and I_1 are the actual voltage and current of #1, V_2 and I_2 are the actual voltage and current of #2, and h is the imbalance factor of the coupled transmission lines and remains constant as long as the cross-sectional structure stays unchanged.

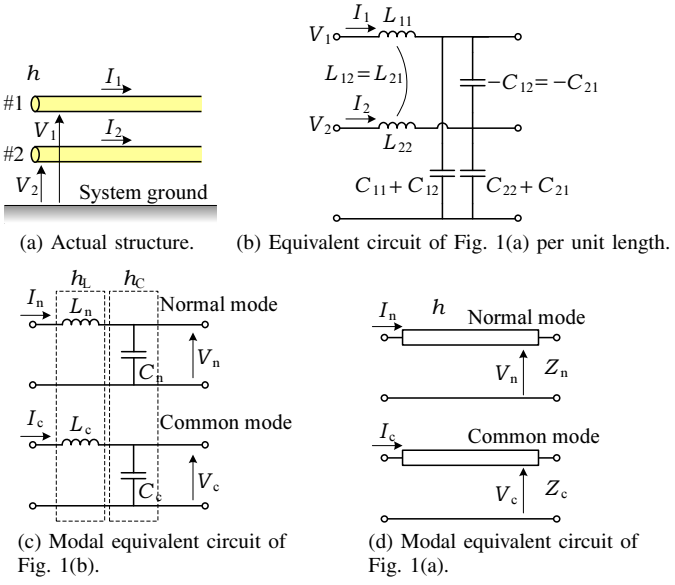

(a) Actual structure.
(b) Equivalent circuit of Fig. 1(a) per unit length.
(c) Modal equivalent circuit of Fig. 1(b).
(d) Modal equivalent circuit of Fig. 1(a).

Fig. 1. Coupled transmission lines and their modal equivalent circuit.

Fig. 1(b) shows the equivalent circuit of Fig. 1(a) per unit length. In Fig. 1(b), L_{11}, L_{12}, L_{21}, and L_{22} are the elements of the inductance matrix and C_{11}, C_{12}, C_{21}, and C_{22} are the elements of the capacitance matrix, which are obtained from a two-dimensional electrostatic calculation in the cross section of the coupled transmission lines. Fig. 1(a) can be expressed by using the cascade connection of a unit shown in Fig. 1(b).

The modal equivalent circuit is provided for each orthogonal mode by applying a mode-decomposition technique to the telegrapher's equations, where the imbalance factor of transmission line h is used. In the mode decomposition from the actual circuit to the modal equivalent circuit, the two relationships between the actual and modal voltages

$$\begin{bmatrix} V_1 \\ V_2 \end{bmatrix} = \begin{bmatrix} 1-h & 1 \\ -h & 1 \end{bmatrix} \begin{bmatrix} V_\mathrm{n} \\ V_\mathrm{c} \end{bmatrix} \quad (1)$$

and between the actual and modal currents

$$\begin{bmatrix} I_1 \\ I_2 \end{bmatrix} = \begin{bmatrix} 1 & h \\ -1 & 1-h \end{bmatrix} \begin{bmatrix} I_\mathrm{n} \\ I_\mathrm{c} \end{bmatrix} \quad (2)$$

are applied, where V_n and I_n are the normal-mode voltage and current including for the general case when $h \neq 0.5$, and V_c and I_c are the common-mode voltage and current.

Now, the mode-decomposition technique provides modal equivalent circuits per unit length that consists of separate circuits of the normal and common modes. Each element of the modal equivalent circuits is characterized by

$$L_\mathrm{n} = L_{11} + L_{22} - 2L_{12}, \quad (3)$$

$$C_\mathrm{n} = \frac{C_{11}C_{22} - C_{12}^2}{C_{11} + C_{22} + 2C_{12}}, \quad (4)$$

$$L_\mathrm{c} = \frac{L_{11}L_{22} - L_{12}^2}{L_{11} + L_{22} - 2L_{12}}, \text{ and} \quad (5)$$

$$C_\mathrm{c} = C_{11} + C_{22} + 2C_{12}. \quad (6)$$

Fig. 1(c) shows a modal equivalent circuit of the unit shown in Fig. 1(b) in the homogeneous transmission lines where h_L=h_C. Then, h_L and h_C can be replaced with the imbalance factor of the coupled transmission lines h. The imbalance factors h_L and h_C are given as

$$h_\mathrm{L} = \frac{L_{22} - L_{12}}{L_{11} + L_{22} - 2L_{12}} \text{ and} \quad (7)$$

$$h_\mathrm{C} = \frac{C_{11} + C_{12}}{C_{11} + C_{22} + 2C_{12}}. \quad (8)$$

When the transmission lines are longitudinally uniform, Fig. 1(c) can be replaced with Fig. 1(d) by using a transmission-line model, where Z_n and Z_c are respectively the normal-mode and common-mode characteristic impedances as

$$Z_\mathrm{n} = \sqrt{\frac{L_\mathrm{n}}{C_\mathrm{n}}} \text{ and} \quad (9)$$

$$Z_\mathrm{c} = \sqrt{\frac{L_\mathrm{c}}{C_\mathrm{c}}}. \quad (10)$$

The current division factor h used as the imbalance factor is defined as the ratio of the common-mode current flowing along #1 to the entire common-mode current. As described earlier, h can be calculated using the inductance and capacitance matrix elements obtained from the two-dimensional electrostatic calculation in the cross section of the transmission lines. Therefore, h is a parameter that indicates the electric-field distribution in the cross section of the transmission lines. The current division factor generally ranges from 0 to 0.5. The factor of balanced (differential) transmission lines such as a two-wire cable is 0.5, whereas that of imbalanced transmission lines is less than 0.5. For example, the current division factors of a coaxial cable and a microstrip line (MSL) are respectively 0 and almost 0.

B. Modal Equivalent Circuit with Mode-conversion Sources

The modal equivalent circuit of the longitudinally uniform transmission lines was explained in the previous section. Let us now focus on the discontinuity formed by connecting two cables with different current division factors, as shown in Fig. 2(a) [4]. Subscripts a and b are used to distinguish two cables with the different current division factors of h_a and h_b, respectively. Fig. 2(b) shows the circuit expression of the modal equivalent circuit of the actual circuit shown in Fig. 2(a) [4]. Fig. 2(b) shows that a current-controlled current source is inserted into the normal-mode circuit and a voltage-controlled voltage source is inserted into the common-mode circuit so that the following relationship holds at the interface:

$$I_\mathrm{na} = I_\mathrm{nb} + \Delta h I_\mathrm{c} \text{ and} \quad (11)$$

$$V_\mathrm{ca} = V_\mathrm{cb} - \Delta h V_\mathrm{n}, \quad (12)$$

where Δh is the difference between the current division factors of the adjacent cables, that is, $\Delta h = h_\mathrm{b} - h_\mathrm{a}$. As seen in Fig. 2, the modal equivalent circuits are no longer separated but actually merged into one circuit by the inserted controlled sources. This suggests that the cascade connection of cables with different current division factors should cause mode conversion at the interface. Therefore, the controlled sources inserted into the interface was named mode-conversion sources. The mode-conversion current and voltage sources are respectively expressed as the product of Δh and the common-mode current at the interface I_c, and the product of Δh and the normal-mode voltage at the interface V_n.

The modal equivalent-circuit model with mode-conversion sources was validated by conducting a full-wave simulation and measurement in a transmission system where the TEM-mode propagation is satisfied [4], [5].

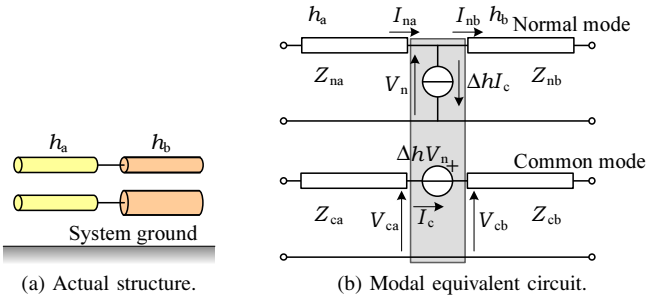

(a) Actual structure. (b) Modal equivalent circuit.

Fig. 2. Cascade connection of two cables with different current division factors of h_a and h_b, and modal equivalent circuit of Fig. 2(a).

C. Modal Equivalent Circuit of Bend Region in Differential Transmission Lines

This section provides the modal equivalent circuit of the bend in the differential transmission lines of interest. Fig. 3(a) shows the right-angled bend. The following discussion is presented on the stripline structure shown in Fig. 3(b) because the modal equivalent circuit assumes a TEM-mode transmission in homogeneous media.

Let us briefly describe the modal equivalent circuit of the straight region before discussing the bend region of the differential transmission lines. The parameters of the modal equivalent circuit are given by the inductance and capacitance matrix elements obtained from the cross-sectional structure of the lines, and then $h = 0.5$ because the widths of the differential transmission lines are equal.

In the bend region shown in Fig. 3(a), the equivalent circuit of the actual structure is written by using a T-type structure of the reactive elements, as shown in Fig. 4(a), because the bend is directionally symmetrical. This paper takes into consideration the equivalent circuit shown in Fig. 4(a), that is, the cascade connection of the inductance region, the capacitance region, and the inductance region, in order. Of course, the equivalent circuit sandwiched by the capacitance regions is also true.

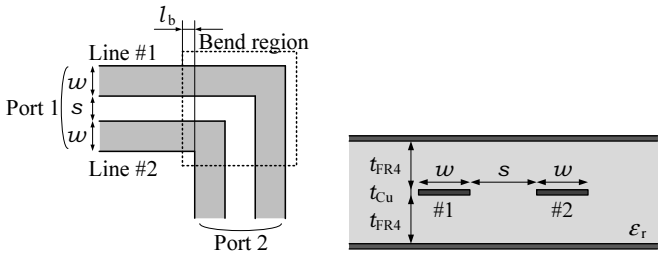

(a) Right-angled bend. (b) Cross section.

Fig. 3. Differential transmission lines and their bend treated in this paper.

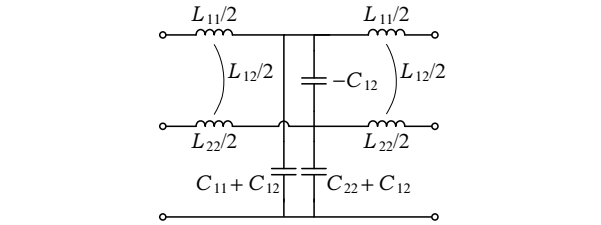

(a) Equivalent circuit.

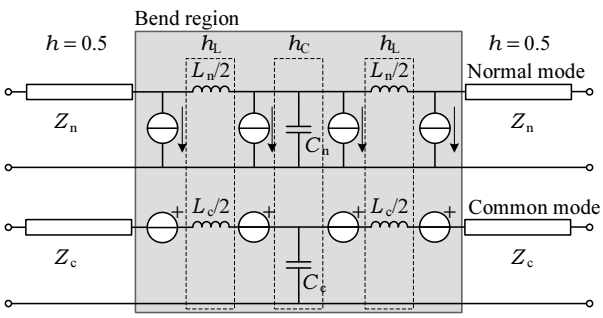

(b) Modal equivalent circuit.

Fig. 4. Comparison between two equivalent-circuit models of bend region in differential transmission lines.

The h_L and h_C current division factors are respectively calculated using (7) and (8) along with the inductance and capacitance matrix elements extracted from the three-dimensional structure of the bend region. Since line #1 is longer than line #2, h_L and h_C are usually unequal in the bend region and the relationship of $h_L < h(= 0.5) < h_C$ holds. This means there is inequality in h_L and h_C, and therefore, the mode-conversion sources should be inserted at the interface in the modal equivalent circuit as described earlier. As a result, we can obtain the modal equivalent circuit of the bend region in the differential transmission lines shown in Fig. 4(b).

Fig. 4(b) shows four sets of mode-conversion sources and the differences in imbalance factors are $h_L-0.5$, h_C-h_L, h_L-h_C, and $0.5-h_L$ in order from the left. In addition, when the directions of the mode-conversion sources are assigned as shown in Fig. 4(b), the difference in adjacent imbalance factors is defined by the subtraction of the value on the left side of the interface from the value on the right side. Therefore, note that the difference value may be negative. The adjacent mode-conversion sources are usually connected out of phase of each other but they are not completely cancelled because the reactive elements between them change the phase depending on the frequency.

III. Model Validation

A. Physical Parameters

The modal-equivalent circuit model proposed in the previous section is validated using two types of the right-angled bends shown in Fig. 3(a).

Table I summarizes the physical parameters of the differential transmission lines used for model validation. The common physical parameters of the cross section shown in Fig. 3(b) are t_{FR4}=100 μm and t_{Cu} =18 μm. The dielectric is assumed to be glass epoxy and ε_r= 4.4. The differential-mode characteristic impedances of both types are set to 100 Ω. Since the coupling coefficients of Models A and B are respectively 0.035 and 0.25, Model B is more tightly coupled than Model A. We have used normal mode as the general expression including $h \neq 0.5$ thus far, but let us use the expression differential mode for the input-output evaluation in the following.

For the input-output evaluation, the mixed mode S parameter is used when the straight regions of 35 mm on the input side and 25 mm on the output side are connected to the bend. The circuit simulation using the modal equivalent circuit was carried out by AWR Microwave Office after a 2D Extractor and Q3D Extractor were used for the parameter extraction from the straight region (cross section) and the bend region in the differential transmission lines, respectively. In addition, ANSYS HFSS was used as a reference for the model validation. All the simulations were carried out assuming no material loss.

TABLE I. Physical parameters of differential transmission lines used for model validation.

Item	Model A	Model B
s (μm)	180	60
w (μm)	70	30

B. Model Validation Focusing on Bend Region

Fig. 5 shows the magnitude of S_{cd21} obtained by conducting a circuit simulation using the modal equivalent circuit in comparison with full-wave simulation as a reference. As seen in the figure, the circuit simulation using the modal equivalent circuit agrees well with the full-wave simulation at l_b= 0.09 mm in Model A and at l_b= 0.14 mm in Model B. As shown in Fig. 3(a), l_b is the effective length to define the bend region in the modal equivalent circuit and an appropriate l_b is required for the circuit simulation using the modal equivalent circuit.

As for Model A, three other conditions, which are l_b= 0.84 mm, 0.34 mm, and 0.02 mm, are also shown in Fig. 5, and it was found that S_{cd21} gets smaller as l_b decreases.

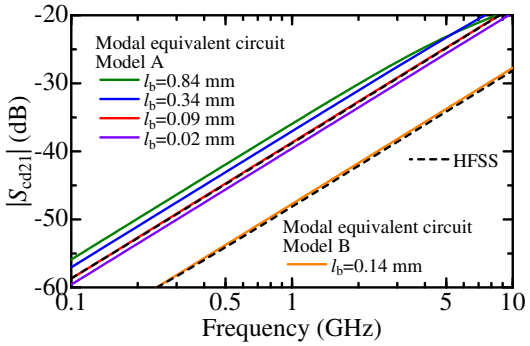

Fig. 5. Comparison of S_{cd21} between circuit simulation with modal equivalent circuit and full-wave simulation.

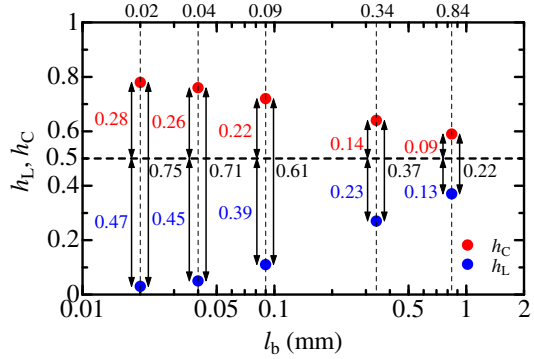

(a) h_L and h_C in terms of l_b.

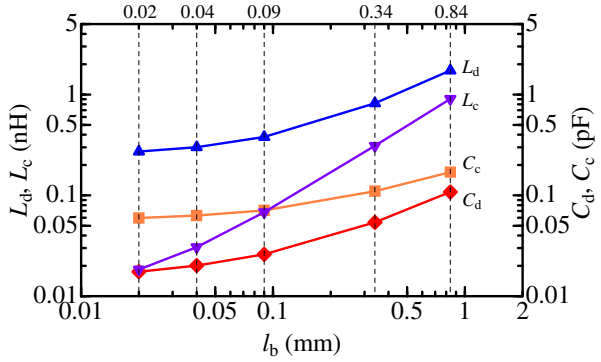

(b) L_d, L_c, C_d, and C_c in terms of l_b.

Fig. 6. Imbalance factor, modal inductance, and modal capacitance as a function of l_b in Model A.

Let us consider the relationship between S_{cd21} and l_b focusing on the current division factors and the reactive elements. First, Fig. 6(a) shows h_L and h_C in terms of l_b and $h_L < h(= 0.5) < h_C$, as predicted earlier. Since the increase in l_b makes the straight region larger in the bend region, both h_L and h_C approach 0.5 and the difference in the imbalance factor is reduced. However, the decrease in Δh suggests that the mode conversion (S_{cd21}) should decrease with l_b and the trend shown in Fig. 5 is completely opposite.

Next, Fig. 6(b) shows the modal inductances L_d and L_c and the modal capacitances C_d and C_c in terms of l_b in Model A. It can be seen from the figure that the differential- and common-mode reactances monotonically increase with l_b. This is because the increase in l_b enlarges the bend region. The modal reactive elements are inserted between the adjacent mode-conversion sources with the opposite phase of each other, and therefore, the larger the modal reactances get, the less they are cancelled. As a result, the modal reactances mainly contribute to the increase in S_{cd21}.

As seen from the above discussion, the difference in the imbalance factors generates mode conversion and then the modal reactances of the bend region enhance it. Therefore, focus must be placed on not only the difference in the imbalance factors but also the modal reactances in the modal equivalent circuit to create a bend with less mode conversion.

IV. Conclusion

The equivalent-circuit expression of the bend discontinuity in the differential transmission lines on printed circuit boards was proposed in this paper from the view of the mode-decomposition technique. We clarified that not only the imbalance factors but also the modal reactances of the bend region largely contribute to the mode conversion.

Acknowledgment

The authors would like to thank Mr. Yuki Yamashita, an undergraduate student at Okayama University, for his contribution to the simulation in this study.

References

[1] Y. Kami, "Transmission-line circuit theory in EMC and its development," *IEICE Trans. Commun.*, vol.J-90B, no.11, pp.1070-1082, Nov. 2007 (in Japanese).

[2] A. Sugiura, and Y. Kami, "Generation and propagation of common-mode currents in a balanced two-conductor line," *IEEE Trans. Electromagn. Compat.*, vol.54, no.2, pp.466-473, Apr. 2012.

[3] H. Uchida, "Fundamentals of coupled lines and multiwire antennas," Sasaki Printing, Sendai, Japan, 1967.

[4] Y. Toyota, K. Iokibe, R. Koga, and T. Watanabe, "Mode-equivalent modelling of system consisting of transmission lines with different imbalance factors," in *Proc. Asia-Pacific Int. Symp. Electromagn. Compat.*, pp.676-679, May 2011.

[5] K. Sejima, Y. Toyota, K. Iokibe, L. R. Koga, and T. Watanabe, "Experimental model validation of mode-conversion sources introduced to modal equivalent circuit," in *Proc. IEEE Int. Symp. Electromagn. Compat.*, pp.492-497, Aug. 2012.

[6] Y. Toyota, K. Iokibe, and T. Watanabe, "Mode Conversion Caused by Discontinuity in Transmission Line: From Viewpoint of Imbalance Factor and Modal Characteristic Impedance,"in *Proc. 2013 IEEE Electr. Design Adv. Packag. Sys. Symp.*, pp.52-55, Dec. 2013.